Physical Properties and Successive Phase Transitions in Quasi-One-Dimensional Sulfides ACu_7S_4 (A = Tl, K, Rb)

T. Ohtani,[1] J. Ogura, H. Yoshihara, and Y. Yokota*

*Laboratory for Solid State Chemistry, and *Research Institute of Natural Sciences, Okayama University of Science, Ridai-cho 1-1, Okayama 700, Japan*

Quasi-one-dimensional sulfides ACu_7S_4 (A = Tl, K) with $(NH_4)Cu_7S_4$-type structure and a new isotypic sulfide $RbCu_7S_4$ were prepared. Thermal analysis, electrical resistivity, thermoelectric power, and magnetic susceptibility measurements showed a large variety of successive phase transitions. The transitions have characteristics common to all three compounds. They are labeled as $T_1(A) \cong$ 395, 445, and 400 K, respectively, for A = Tl, K, and Rb; $T_2(A) \cong$ 245, 250, and 260 K, respectively, for A = Tl, K, and Rb; $T_3(A) \cong$ 220 K for all the compounds; $T_4(A) \cong$ 190, 180, and 190 K, respectively for A = Tl, K, and Rb; $T_5(A) \cong$ 160–170 K for both A = Tl and Rb; $T_6(A) \cong$ 60 K for all the compounds; and $T_7(Rb) \cong$ 30 K. Electron diffraction measurements of KCu_7S_4 showed two kinds of superstructures below $T_2(K)$ and $T_4(K)$, which are characterized by the corresponding commensurate wave vectors $q = \frac{1}{2}c^*$ and $q = \pm(\frac{1}{3}a^* + \frac{1}{3}b^*) + \frac{2}{3}c^*$, respectively. $TlCu_7S_4$ showed the superstructure with $q = \frac{1}{2}c^*$ below $T_2(Tl)$ and one with $q = \frac{1}{2}(a^* + b^*) + \frac{1}{3}c^*$ on further cooling. $RbCu_7S_4$ showed only $q = \frac{1}{2}c^*$ below $T_2(Rb)$. An order-disordering mechanism was proposed to be the possible origin for the transition $T_2(A)$. The origins of the other transitions are not clear. Through studies on nonstoichiometric samples, it was revealed that the relatively high conductivity of these compounds originates from the atomic vacancies of both Cu and Tl. © 1995 Academic Press, Inc.

INTRODUCTION

In the past two decades, a large number of quasi-one-dimensional compounds have been intensively investigated. These efforts have been devoted mainly to two subjects: one is the search for new types of superconducting materials with a high critical temperature T_c based on an excitonic mechanism (1), and the other is research on charge-density-wave (CDW) instability (2). Although the candidates for excitonic superconductors have not yet been identified, many compounds exhibit the CDW instability, e.g., $NbSe_3$ (2, 3), $(NbSe_4)_{10/3}I$ (2, 4), $A_{0.30}MoO_3$ (A = K, Rb, Tl) (2, 5), Nb_3Te_4 (6, 7), $In_xNb_3Te_4$ (8), etc.

Berger and Sobott found a quasi-one-dimensional sul-

fide, $TlCu_7S_4$ (9), which is isostructural with $(NH_4)Cu_7S_4$ as reported by Gattow (10). Recently, we reported a new isotypic sulfide, KCu_7S_4 (11). Figure 1 is a schematic drawing of the structure of ACu_7S_4 (A = NH_4, Tl, K) (11); the unit cell is tetragonal, with symmetry $I\bar{4}$ containing 2 formula units. There are two kinds of Cu sites, labeled as Cu1 and Cu2, which belong to the different 8g sites. The Cu1 atoms are coordinated triangularly to form $[Cu_4S_4]$ columns running parallel to the c axis, and the Cu2 atoms are nearly 3-coordinated and form double "CuS3" tetrahedral chains, which will be referred to as "tetrahedral chains" according to the notation adopted by Whangbo and Canadell (12). The occupancy factor of the Cu2 atoms is $\frac{3}{4}$. The $[Cu_4S_4]$ columns are joined by the tetrahedral chains to form tunnels containing the A ions, which are in the special positions 2c and are surrounded by tetragonal pseudo-cubic prisms of S atoms.

We previously reported the temperature variations of the resistivity ρ of $TlCu_7S_4$ associated with three phase transitions at 160–170, 190–200, and 240–250 K, and those of KCu_7S_4 with two phase transitions at 175–190 and 240–250 K (11). Both compounds have relatively low resistivity on the order of 10^{-2}–10^{-1} $\Omega \cdot$ cm in spite of the filled bands of the d^{10} state of Cu^+. Thermoelectric power and magnetic susceptibility measurements also showed anomalies at the corresponding temperatures. It is of considerable interest that the present compounds resemble $K_3Cu_8S_6$, which contains similar $[Cu_4S_4]$ chains and the tetrahedral chains and shows CDW-like anomalies at ~153 and 55 K (13–17). On the basis of band calculation using the extended Hückel tight-binding method, Whangbo and Canadell claimed that the transitions in $TlCu_7S_4$ and $K_3Cu_8S_6$ cannot originate from the CDW instabilities, but are caused by an order–disorder transition of the Cu^+ ions in the tetrahedral chains (12).

However, the origins of the phase transitions as well as of the relatively high conductivity are not entirely clear. In the present work, therefore, we performed more detailed investigations on $TlCu_7S_4$, KCu_7S_4, and a new isotypic sulfide, $RbCu_7S_4$, through powder X-ray diffraction,
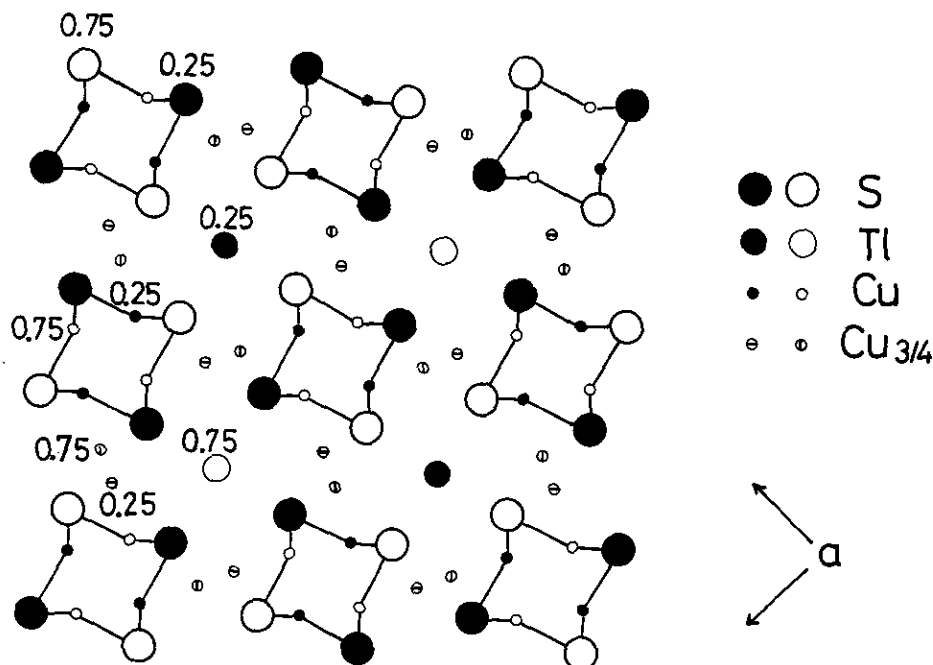
379

FIG. 1. Schematic crystal structure of $ACu_7S_4(A = Tl, K)$ with $(NH_4)Cu_7S_4$ type. The unit cell is tetragonal with symmetry $I\bar{4}$.

DTA (differential thermal analysis), DSC (different scanning calorimetry), electrical resistivity, thermoelectric power, magnetic susceptibility, and electron diffraction measurements.

EXPERIMENTAL

$TlCu_7S_4$ and KCu_7S_4 were obtained by heating mixtures of the elements Tl (or K), Cu, and S in the stoichiometric ratio in evacuated silica tubes. To prevent the reaction of Tl (or K) with humidity and oxygen, the starting mixtures were treated in a dry box under a purified nitrogen atmosphere. The mixtures were heated up to 1073 K at a rate of 100 K/hr, and then annealed at 673 K for 1 week. The obtained specimens were pelletized and sealed again in silica tubes, and then were sintered at 573 K for $TlCu_7S_4$ and at 673 K for KCu_7S_4 for 1 week. $RbCu_7S_4$ was prepared from a mixture of the desired ratio of RbS, Cu, and S in the same way as used for the preparation of KCu_7S_4. RbS was separately prepared in the following manner. Commercially available Rb metal, sealed in a Pyrex glass ampule, was sealed into a silica tube together with an equimolar amount of S powder, and then the glass ampule was broken inside the silica tube, followed by heating at 573 K for 2 weeks. X-ray powder diffraction measurements were performed at room temperature using a diffractometer RIGAKU RAD-B. Intensity data were collected with $CuK\alpha$ radiation at 0.05° intervals, and the data were analyzed by Rietveld refinement using a RIETAN program (18). DTA measurements were performed from

room temperature to 1000 K by using MAC SCIENCE TG-DTA 2000; samples were sealed into a small silica tube with a thin bottom especially designed for good thermal contact with the sample holder. DSC measurements were carried out from ~100 to 300 K using MAC SCIENCE DSC-3100. Both of the thermal measurements were performed at heating and cooling rates of 10 K/min. Electrical resistivity ρ was measured using an ordinary dc four-probe method from 3 to 273 K. Thermoelectric power (Seebeck coefficient S) measurements were performed from ~100 to 273 K using Cu leads with a temperature gradient of ~0.3 K/cm. Magnetic susceptibility χ was measured from 4.2 to 273 K using a Faraday-type magnetic balance (Oxford Instruments Ltd., System: RS177D + CF1200S + ADAS). All the measurements of ρ, S, and χ were carried out on cooling and subsequently on heating. Electron diffraction measurements were performed from room temperature down to ~30 K using a JEM-2000EX electron microscope.

RESULTS

Structure

All the compounds were obtained as a black powder, and were quite stable in air. The powder X-ray diffraction patterns indicated that all the compounds have the $(NH_4)Cu_7S_4$-type structure. The reproducibility was much higher than in the earlier report (9). The lattice parameters obtained by the least-squares method are $a = 10.174(4)$
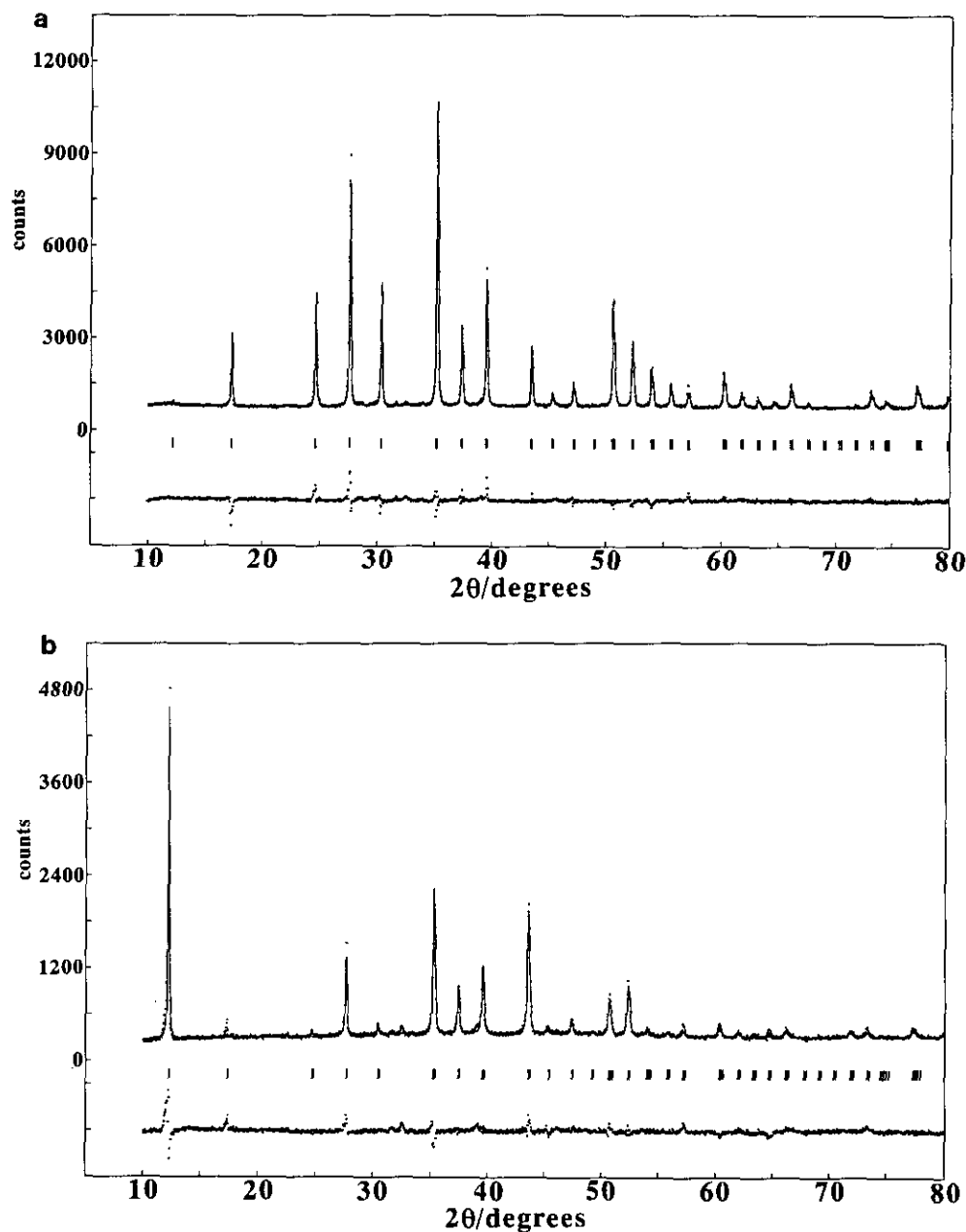
FIG. 2. Profile fits of powder X-ray diffraction patterns obtained by Rietveld analysis of $TlCu_7S_4$ (a) and KCu_7S_4 (b).

Å and $c = 3.8389(2)$ Å for $TlCu_7S_4$, $a = 10.163(5)$ Å and $c = 3.8380(4)$ Å for KCu_7S_4, and $a = 10.271(5)$ Å and $c = 3.8396(3)$ Å for $RbCu_7S_4$. The lattice parameters increase according to the increase of the ionic radius r of A^+, i.e., $r(K^+) = 1.33$ Å, $r(Tl^+) = 1.47$ Å, and $r(Rb^+) = 1.48$ Å. The expansion of the c axis is smaller than that of the a axis because the tunnels run along the c axis.

The starting model for the Rietveld analysis was derived from the structure of $(NH_4)Cu_7S_4$ (space group $I\bar{4}$) (10) by replacing $(NH_4)^+$ with A^+. The profile fits for $TlCu_7S_4$ and KCu_7S_4 are shown in Figs. 2a and 2b, respectively.

The calculated profile plots agree well with the observed patterns for both cases. Although the X-ray pattern of $RbCu_7S_4$ is close to those of both $TlCu_7S_4$ and KCu_7S_4, the Rietveld analysis did not give reasonable R values, presumably due to the presence of a small amount of impurities and to the relatively weak intensity of the diffraction peaks. Table 1 shows the positional parameters and isotropic thermal parameters of four atoms for $TlCu_7S_4$ and KCu_7S_4. The final R factors are $R_{wp} = 5.2\%$, $R_p = 3.6\%$, $R_B = 5.9\%$, $R_F = 3.1\%$, and $R_e = 3.2\%$ for $TlCu_7S_4$, and $R_{wp} = 7.9\%$, $R_p = 5.5\%$, $R_B = 9.5\%$, $R_F =$

TABLE 1
Positional Parameters and Equivalent Isotropic Thermal Parameters

Atoms	x	y	z	$U_{eq}(\text{Å}^2)^a$	occ.[b]
			⟨TlCu₇S₄⟩		
Tl	0	0	0	1.55(4)	1.0
Cu1	0.022(2)	0.361(8)	−0.034(7)	1.08(6)	1.0
Cu2	0.175(7)	0.270(2)	0.532(8)	6.49(7)	0.75
S	0.239(2)	0.429(2)	−0.047(1)	2.07(3)	1.0
			⟨KCu₇S₄⟩		
K	0	0	0	3.65(2)	1.0
Cu1	0.027(8)	0.356(1)	0.026(4)	0.96(9)	1.0
Cu2	0.163(6)	0.258(3)	0.468(1)	2.25(6)	0.75
S	0.259(1)	0.451(4)	−0.078(9)	5.30(2)	1.0

^{a} $U_{eq} = (8\pi^2/3) \Sigma_i \Sigma_j U_{ij} a_i^* a_j^* \mathbf{a}_i \cdot \mathbf{a}_j$.

^{b} Site occupancy.

7.1%, and $R_e = 5.1\%$ for KCu₇S₄. The atomic positions in both compounds are close to those in $(NH_4)Cu_7S_4$, while, as opposed to the original determination of $z = 0.35(10)$, the Cu2 atoms are situated near the ideal position of $z = \frac{1}{4}$ in both TlCu₇S₄ and KCu₇S₄. The high U_{eq} value for C2 site in TlCu₇S₄ implies that the site occupancy factor is not just 0.75, but probably less than 0.75. However, the value of U_{eq} was not remarkably improved by adopting the occupancy factor smaller than 0.75. The typical interatomic distances are given in Table 2 for both TlCu₇S₄ and KCu₇S₄. Although the lattice parameters of TlCu₇S₄ are larger than those of KCu₇S₄, the averaged interatomic distances of Cu1–Cu1, Cu1–S, and S–S within the [Cu₄S₄] columns in TlCu₇S₄ are smaller than those in KCu₇S₄. On the other hand, the values of the S–S (intercolumn) and the A–S distances in TlCu₇S₄ are larger than those in KCu₇S₄. These results clearly show that the cross section of the [Cu₄S₄] columns in TlCu₇S₄

TABLE 2
Selected Bond Length (Å) of TlCu₇S₄ and KCu₇S₄

	TlCu₇S₄	KCu₇S₄
Cu1–Cu1	2.606(2×), 2.972(2×), 2.848	2.717(2×), 2.990(2×), 2.979
Cu1–S	2.128, 2.312, 2.635	2.219, 2.574, 2.544
S–S (intracolumn)	3.839, 3.905	3.838, 3.584
(intercolumn)	3.913	4.014
S–Tl (or K)	3.253(8×)	2.975(8×)
Cu2–S	2.827, 2.227, 4.442, 2.374	2.311, 2.650, 2.171, 4.100
Cu2–Cu2	2.478(2×)	2.607(2×)
Cu2–Cu1	2.462, 2.593, 2.838, 2.929, 2.939	2.548, 2.580, 2.756, 3.345, 3.813

is smaller than in KCu₇S₄, indicating that the columns are well isolated in TlCu₇S₄ compared with those in KCu₇S₄. In the tetrahedral chains, the Cu2–S distances are 2.227, 2.510 (within the a–b plane), and 2.374 Å (between the neighboring a–b planes) for TlCu₇S₄, and are 2.311, 2.171, and 2.650 Å for KCu₇S₄, respectively. Consequently the Cu2–Cu2 distance is shorter in TlCu₇S₄ (=2.478 Å) than in KCu₇S₄ (=2.607 Å). The Cu2–Cu2 distance in TlCu₇S₄ is a reasonable value for the Cu⁺–Cu⁺ distance (19).

Eriksson et al. reported that TlCu₇Se₄ has also the $(NH_4)Cu_7S_4$ structure, but the space group is $I4/m$ rather than $I\bar{4}$ (20). We thus performed a Rietveld analysis in the space group $I4/m$ for both TlCu₇S₄ and KCu₇S₄. The results for KCu₇S₄ showed the large divergence, which suggests that the favorable space group for this compound is $I\bar{4}$. On the other hand, the obtained R factors for TlCu₇S₄ were comparable to those obtained in the space group $I\bar{4}$. For the following two reasons, we speculate that the space group $I\bar{4}$ is much preferable to $I4/m$ for TlCu₇S₄: (a) our preliminary preparation of the system $TlCu_7(S_{1-x}Se_x)_4$ showed a two-phase region in the range $0.6 \leq x \leq 0.9$, suggesting the space groups are different between TlCu₇S₄ and TlCu₇Se₄; and (b) the system $(Tl_{1-x}K_x)Cu_7S_4$ ($0 \leq x \leq 1.0$) showed a complete solid solution, which will be mentioned in the later section. For further clarification, however, the more precise structure analyses should be performed by using single crystals.

Thermal Analysis

DTA measurements revealed that TlCu₇S₄ melts incongruently at 690–730 K, and that KCu₇S₄ and RbCu₇S₄ melt nearly congruently at 905 and 925 K, respectively. A small endothermic peak was observed at ~395, ~445, and ~400 K upon heating, respectively, for TlCu₇S₄, KCu₇S₄ and RbCu₇S₄, and on cooling at ~365 K for TlCu₇S₄. The results of DSC measurements below room temperature are as follows. TlCu₇S₄ has endothermic peaks at 170, 196, and 220 K on heating, and exothermic peaks at 160 and 193 K on cooling. The latent heat of the 196-K transition is 0.250 J/g, while that of the other transitions is too weak to be estimated. KCu₇S₄ exhibits the endothermic peak at 186 K on heating, and the exothermic peak at 181 K on cooling; the latent heat of the endothermic peak is 0.212 J/g, whereas it is 1.89 J/g for the exothermic peak. RbCu₇S₄ shows endothermic peaks at 180, 196, and 248 K on heating, and exothermic peaks at 191 and 242 K on cooling. The latent heat of the endothermic peak at 196 and 248 K is 0.689 and 0.0438 J/g, respectively.

Transport Properties

Figure 3 shows temperature variations of the resistivity ρ of ACu_7S_4 (A = Tl, K, Rb). The resistivity of TlCu₇S₄
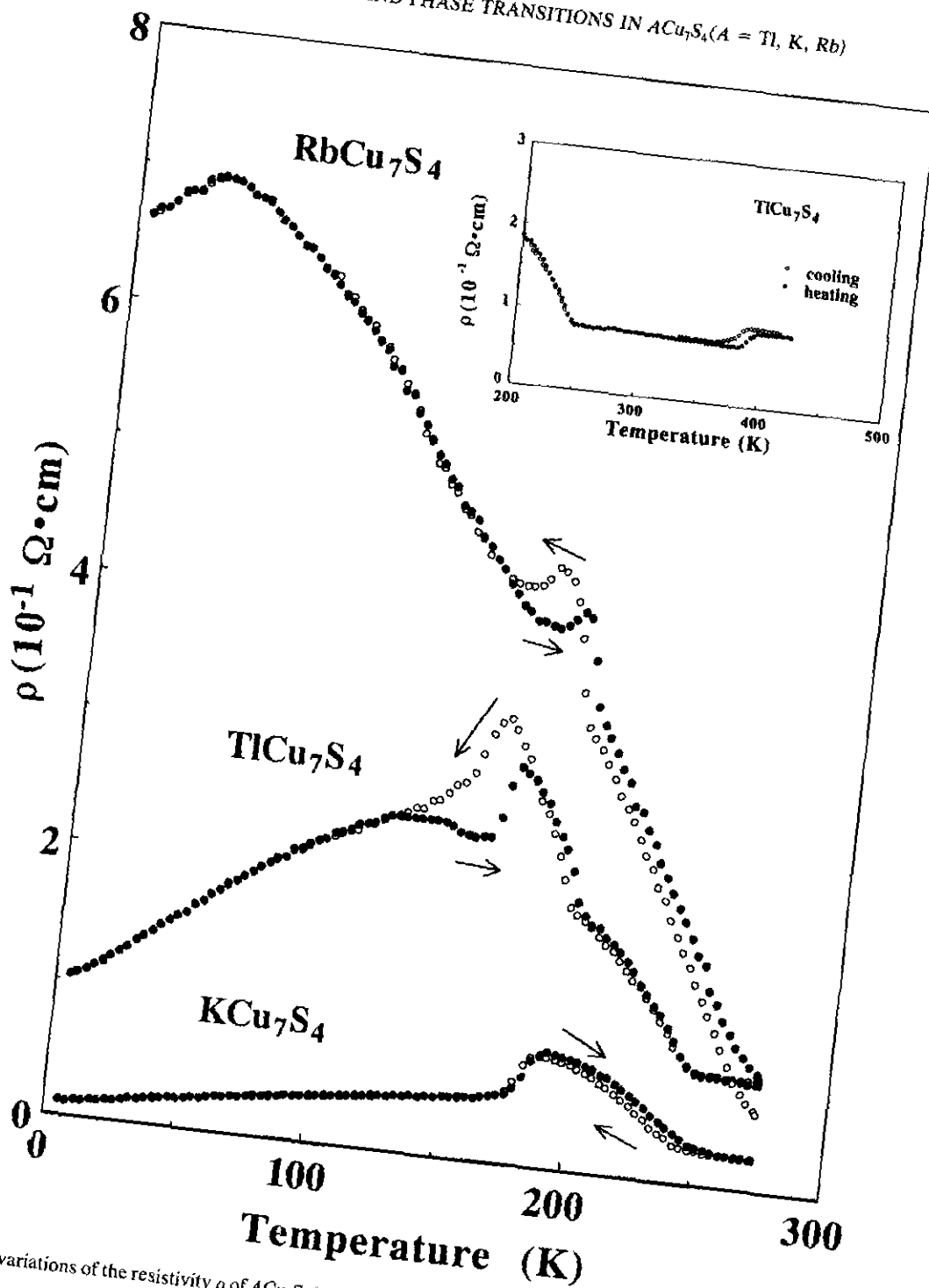
FIG. 3. Temperature variations of the resistivity ρ of $ACu_7S_4 (A = Tl, K, Rb)$. The inset gives the resistivity of $TlCu_7S_4$ in the higher temperature range up to 425 K.

increases with decreasing temperature, indicative of semi-conductive behavior down to ~160 K, and exhibits the distinct bends at ~245 and ~190 K. Upon further cooling, the resistivity shows a drop at ~160 K, and tends to show metallic conduction down to 3K. A large hysteresis was observed in the temperature range between ~120 and

~190 K. The resistivity of KCu_7S_4 shows semiconductive behavior on cooling from 273 to ~180 K, and exhibits a bend at ~250 K, and the resistivity tends to show metallic behavior down to 3 K via a sudden decrease at ~180 K. A small hysteresis was observed between ~180 and ~250 K. The resistivity of $RbCu_7S_4$ shows semiconductive be-

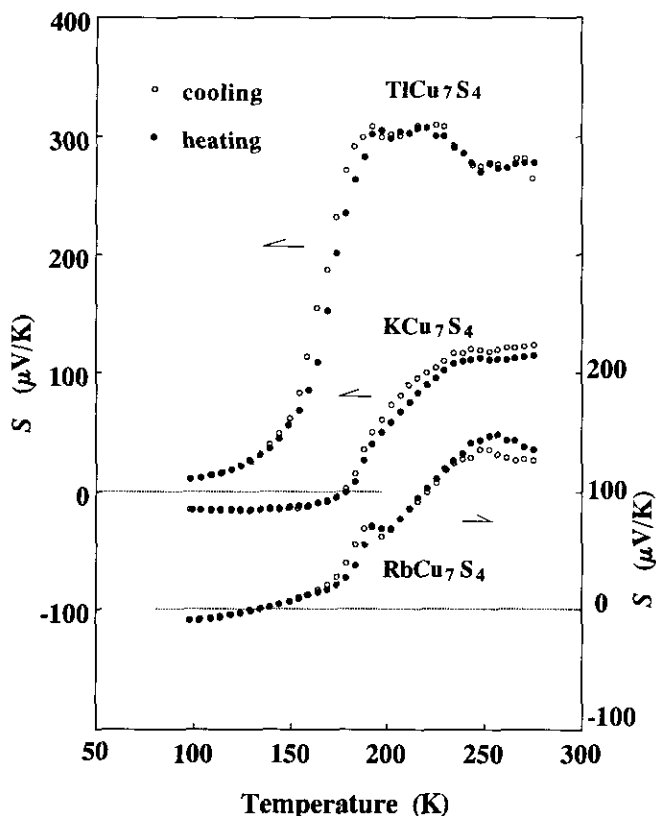FIG. 4. Temperature variations of Seebeck coefficients S for $A\mathrm{Cu_7S_4}(A = \mathrm{Tl, K, Rb})$.

recognized at $\sim$190, $\sim$225, or $\sim$245 K. The S values of $\mathrm{KCu_7S_4}$ show a small hump at $\sim$245 K and then decrease with decreasing temperature down to about 100 K, and exhibits a distinct drop at $\sim$180 K. The most characteristic feature for $\mathrm{KCu_7S_4}$ is that the sign of S changes from positive to negative at $\sim$175 K with decreasing temperature, which is simply considered that the dominant carriers change from holes to electrons near this temperature. The S–T curve of $\mathrm{RbCu_7S_4}$ has a broad maximum at $\sim$250 K, and an obvious hump at 180–200 K corresponding to the hump in the ρ–T curve. $\mathrm{RbCu_7S_4}$ also exhibits a change of sign of S from positive to negative with decreasing temperature around 130 K.

Magnetic Susceptibility

In the temperature range below $\sim$150, $\sim$175, and $\sim$180 K, respectively, for $\mathrm{TlCu_7S_4}$, $\mathrm{KCu_7S_4}$, and $\mathrm{RbCu_7S_4}$, the values of magnetic susceptibility χ were well fitted to a Curie–Weiss law $\chi = \chi_0 + C/(T - \theta)$, where χ_0 is a temperature-independent term, C is a Curie constant, and θ is a Weiss constant. Figure 5 gives temperature dependences of inverse magnetic susceptibility $(\chi - \chi_0)^{-1}$ for $A\mathrm{Cu_7S_4}$ (A = Tl, K, Rb). One can notice a slight change of the slope of the $(\chi - \chi_0)^{-1}$ vs T curve at $\sim$60 K for
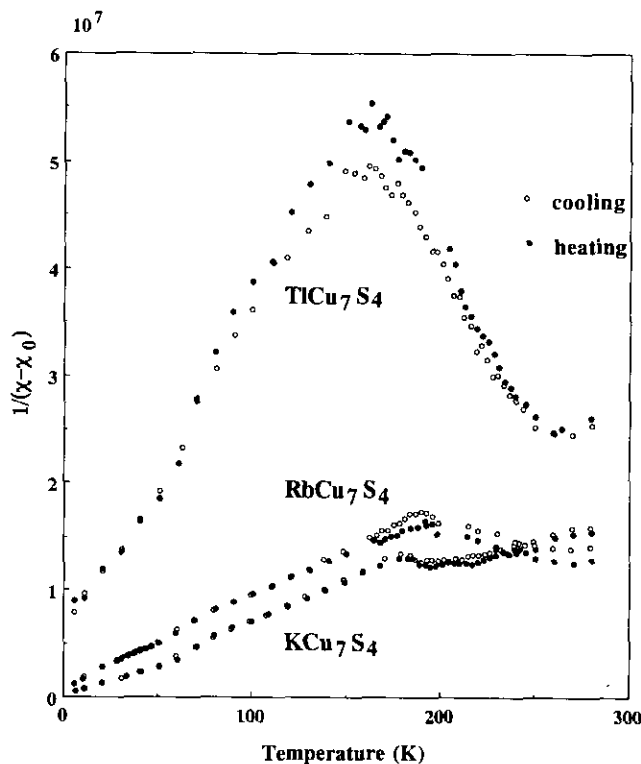
havior down to $\sim$30 K with exhibiting a small bend at $\sim$260 K and an obvious hump at $\sim$180 K, and then shows metallic behavior below $\sim$30 K. A large hysteresis was observed in the temperature range 160–190 K, and the temperature dependence of ρ is irreversible above $\sim$190 K. The inset gives the resistivity of $\mathrm{TlCu_7S_4}$ in the higher temperature range up to 425 K. A distinct anomaly is observed at 360–400 K accompanied by a hysteresis, which definitely corresponds to the anomaly observed in the DTA measurements. Similar anomalies also were observed in $\mathrm{KCu_7S_4}$ and $\mathrm{RbCu_7S_4}$ at the temperatures corresponding to the anomalies observed in the DTA measurements. All the results of ρ measurements above mentioned were quite reproducible. No superconductivity was obseved above 3 K in any of the compounds.

Temperature variations of Seebeck coefficients S for $A\mathrm{Cu_7S_4}$ (A = Tl, K, Rb) are given in Fig. 4. The values of S of $\mathrm{TlCu_7S_4}$ are of the order of $\sim$300 μV/K in the temperature range between $\sim$190 and 273 K, with these values being compatible with the semiconductive nature as observed in the ρ measurements. In the range of 150–190 K, the values of S shows a drastic decrease with decreasing temperature down to $\sim$20 μV/K, which corresponds to the sharp drop in ρ. The other anomalies are

FIG. 5. Temperature variations of the inverse magnetic susceptibility $(\chi - \chi_0)^{-1}$ for $\mathrm{TlCu_7S_4}$, $\mathrm{KCu_7S_4}$, and $\mathrm{RbCu_7S_4}$, where χ_0 is a temperature-independent term of the magnetic susceptibility χ.

each compound, suggesting a new phase change. Further, it is notable that $RbCu_7S_4$ shows an obvious anomaly at about 30 K, suggesting a transition, which appears to correspond to the maximum in the $\rho-T$ curve. The magnetic parameters estimated from the slopes above ~60 K are $\theta = -11.4$ K, $P_{eff} = 0.053$ μ_B for $TlCu_7S_4$, $\theta = 15.2$ K, $P_{eff} = 0.092$ μ_B for KCu_7S_4, and $\theta = -11.2$ K, $P_{eff} = 0.094$ μ_B for $RbCu_7S_4$, where the P_{eff} is an averaged effective paramagnetic moment per one Cu atom. The slopes below ~60 K for every compound give the slightly smaller values of P_{eff} compared with the above corresponding values. The temperature variations of $(\chi - \chi_0)^{-1}$ in the higher temperature range do not show Curie–Weiss-like behavior, suggesting complex magnetic states presumably due to the existence of many transitions in this temperature range.

Electron Diffraction

Figure 6 gives electron diffraction (ED) patterns of KCu_7S_4 taken at room temperature (a), at ~210 K (b), and at ~100 K (c). The incident electron beam is a direction of $[2\bar{2}0]$. Figure 7 shows the schematic drawing of the ED patterns of KCu_7S_4. Two types of superstructures were observed respectively at ~210 and ~100 K. The superlattice reflections observed at ~210 K are characterized by a commensurate wave vector of $q = \frac{1}{2}c^*$, whose appearance is considered to be associated with the 250 K transition. The additional satellite spots, as shown in Fig. 6c, appeared below 180 K transition. This pattern is characterized by the commensurate wave vectors of $q = \pm (\frac{1}{3}a^* + \frac{1}{3}b^*) + \frac{2}{3}c^*$. The diffraction patterns observed by the other directions of incident beam were all compatible with these q vectors. $TlCu_7S_4$ also showed similar types of satellite patterns, though the patterns are not so clear. The c axis was doubled below the 245 K transition, and additional satellite patterns were observed below ~85 K, which are characterized by the commensurate wave vector of $q = \frac{1}{2}(a^* + b^*) + \frac{1}{3}c^*$. Although it was difficult to observe this pattern above ~85 K, presumably because the satellite spots were too weak, this pattern is assumed to appear below the 190 K or the 160 K transition. $RbCu_7S_4$ showed satellite spots with the wave vectors $q = \frac{1}{2}c^*$ below ~250 K like Tl and K compounds. But no additional satellites were observed down to ~30 K. The satellite spots of $q = \frac{1}{2}c^*$ in $RbCu_7S_4$ disappeared when the samples were heated up to a temperatures higher than ~310 K, which is consistent with the large hysteresis in ρ in this temperature range.

DISCUSSION

Transport

As mentioned before (see the introduction), it is of particular interest that the present compounds show good

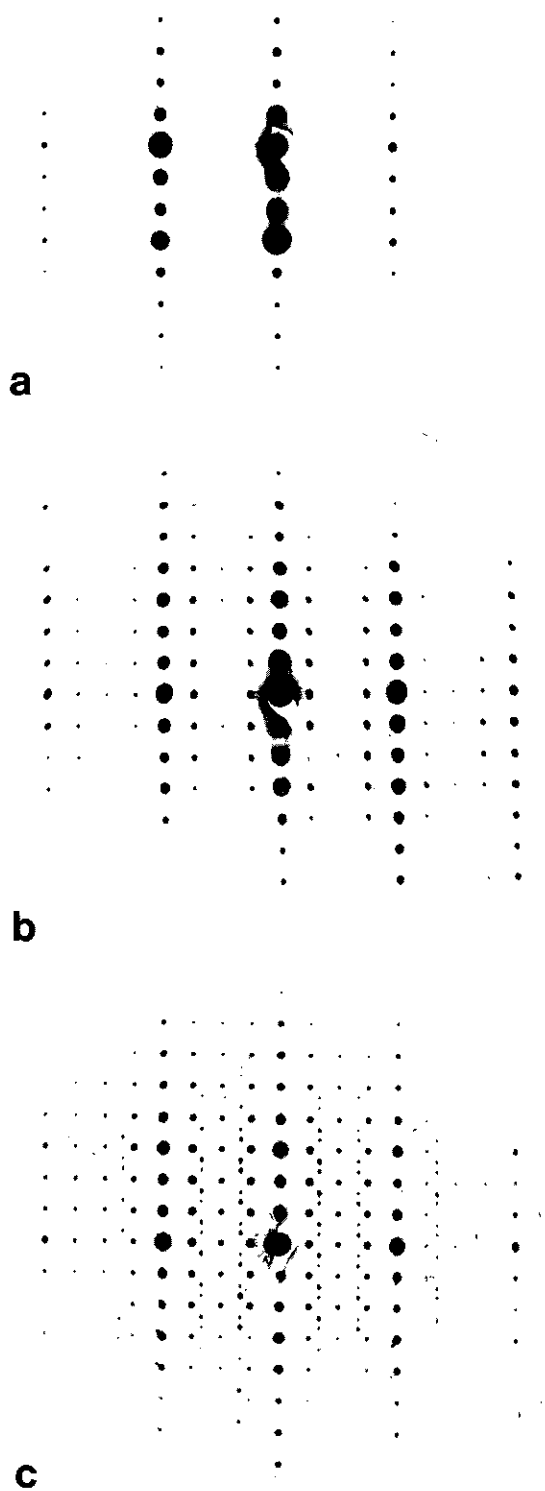FIG. 6. Electron diffraction patterns of KCu_7S_4 taken at room temperature (a), at ~210 K (b), and at ~100 K (c). The incident electron beam is the direction of $[2\bar{2}0]$.
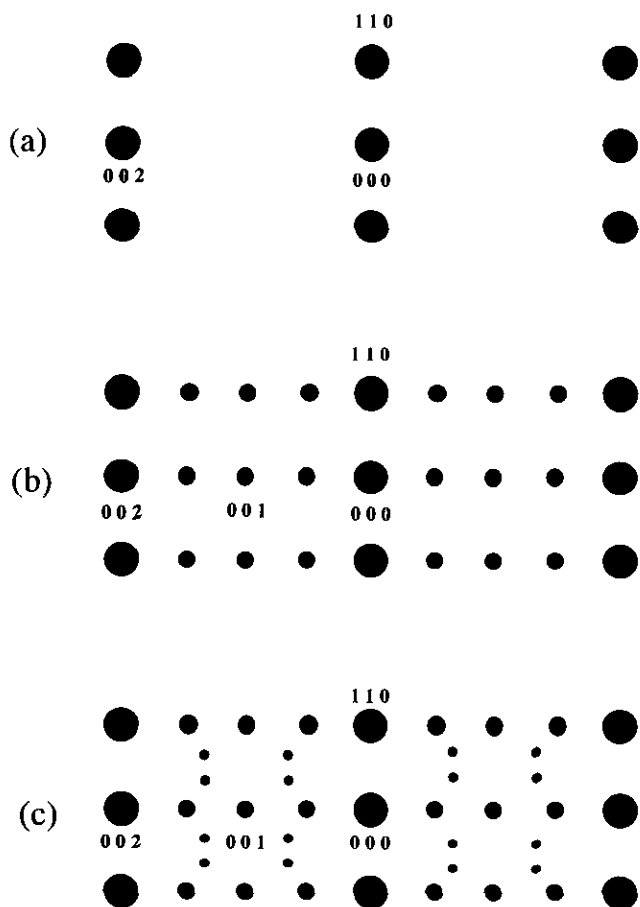
FIG. 7. Schematic drawing of the electron diffraction patterns of KCu7S4 observed at room temperature (a), at ~210 K (b), and at ~100 K (c).

conductivity in all temperature ranges down to 3 K in spite of the filled bands of the d^{10} state of Cu^+. It is most likely that good conductivity is due to the presence of vacancies. Whangbo and Canadell proposed that the compounds have vacancies such that the true formula is represented by $A_{1-x}Cu_{3-y}(Cu_4S_4)$ ($x \neq 0$, $y \neq 0$), and thus sulfur p-block bands of the $[Cu_4S_4]$ columns are partially empty, leading to the metallic character (12). This speculation is supported by the present results of the positive Seebeck coefficients above ~100 K, which suggest the presence of holes originating from the cation vacancies. Further, one should note the presence of magnetic moments for all the compounds. It is most plausible to suppose that the magnetic moments arise from the Cu^{2+} ions generated by the Cu vacancies, because the starting element of Cu is 99.9% pure, and both A (A = Tl, K, Rb) and S scarcely contain magnetic impurities. Based on this assumption, the number of Cu^{2+} ions was estimated to be 0.092%, 0.28%, and 0.29% of the total number of Cu atoms, respectively, for $TlCu_7S_4$, KCu_7S_4, and $RbCu_7S_4$. As currently

recognized, the copper atoms are in the monovalent state in all the chalcogenides, as first proposed by Folmer and Jellinek through X-ray photoelectron spectroscopy studies (21). The present results, however, suggest that the existence of Cu^{2+} ions in the chalcogenides cannot be entirely excluded. From these results, one can suppose that a small number of copper vacancies exist even in the stoichiometric samples in the present compounds.

To clarify the relation between conduction and vacancies, nonstoichiometric samples of the Cu-excess system $TlCu_{7+x}S_4$ ($0 < x \leq 0.20$), the Cu-deficient system $TlCu_{7-x}S_4$ ($0 < x \leq 0.05$), and the Tl-deficient system $Tl_{1-x}Cu_7S_4$ ($0 < x \leq 0.10$) were prepared in the same ways as the stoichiometric samples. All the obtained specimens were of a single phase, and the lattice parameters vary continuously with composition. The excess Cu atoms in the $TlCu_{7+x}S_4$ samples were revealed by Rietveld analysis to be situated at the Cu2 sites. Figure 8 gives the temperature variations of ρ for the variable composition of Cu samples $TlCu_{7+x}S_4$ ($-0.05 \leq x \leq 0.10$). The Cu-deficient samples are more conductive than the stoichiometric sample, whereas the Cu-excess samples are less conductive. Figure 9 shows the temperature dependences of S of the variable composition of Cu samples $TlCu_{7+x}S_4$ ($-0.05 \leq x \leq 0.10$). The sign of S is positive in the measured temper-
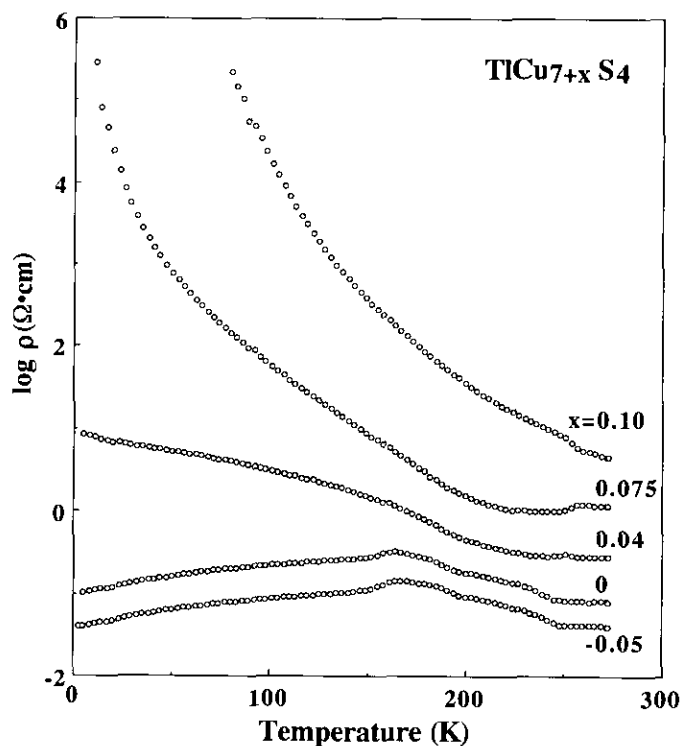

FIG. 8. Temperature variations of the resistivity ρ for the variable Cu composition samples of $TlCu_{7+x}S_4$ ($-0.05 \leq x \leq 0.10$). For simplicity, only the results on cooling are shown.
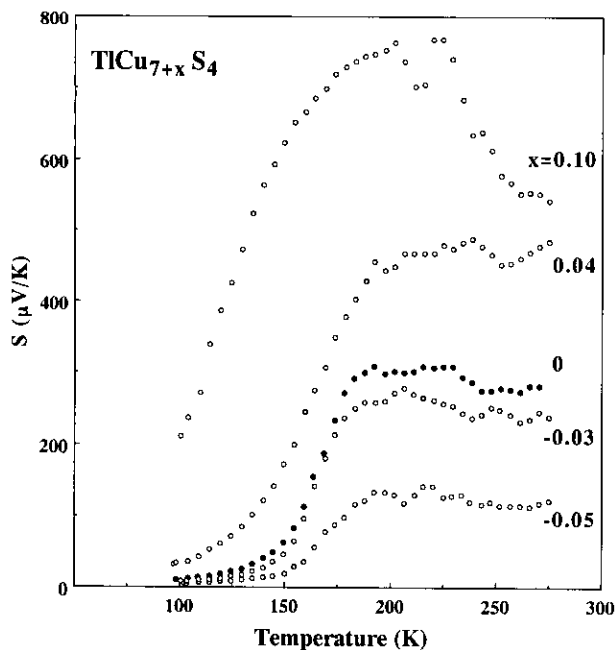
FIG. 9. Temperatue variations of Seebeck coefficient S for the variable Cu composition samples of $TlCu_{7+x}S_4$ ($-0.05 \leq x \leq 0.10$). For simplicity, only the results on cooling are shown.

ature range for all the compositions, and the values increase as the Cu content decreases, suggesting that the number of holes decreases with increasing Cu content. A similar tendency was also observed in the $Tl_{1-x}Cu_7S_4$ system ($0 < x \leq 0.10$). From these results, it is clear that the conductive carriers of the holes in the present compounds originate from the partially empty sulfur p-block bands of the $[Cu_4S_4]$ columns which are induced by the Cu vacancies as well as the Tl vacancies, as suggested by Whangbo and Canadell (12). The relatively weak semiconductive behaviors, as well as the positive values of S observed in the Cu-excess samples, would show that the vacancies cannot be entirely eliminated even by the introduction of excess amounts of Cu atoms. This would be the case for the other compounds of ACu_7S_4 (A = K, Rb).

Phase Transitions

The present compounds exhibit many phase transitions. As far as the authors know, such a large variety of successive phase transitions have not yet been found in other compounds. The transitions appear to have common characteristics among the compounds concerning the transition temperatures and the manner of the change of physical properties across the transitions. They can be summarized as: (1) $T_1(A)$: the 396 K, 446 K, and 402 K transitions, respectively, for A = Tl, K, and Rb, as detected by the DTA peaks and the drop in ρ on cooling;

(2) $T_2(A)$: the 245 K, 250 K, and 260 K transitions, respectively, for A = Tl, K, and Rb, which are characterized by the bend in the ρ–T curves; (3) $T_3(A)$: The 220 K transition observed in all the compounds, as detected by the DSC and the S measurements; (4) $T_4(A)$: the 190 K, 180 K, and 190 K transitions, respectively, for A = Tl, K, and Rb, as commonly observed in the change of S and χ across the transitions; (5) $T_5(A)$: the 160–170 K transition for both A = Tl and Rb, which is accompanied by a drop in ρ on cooling and a small DSC peak; (6) $T_6(A)$: the 60 K transition for every compound, which is clearly observed in the χ–T curves; and (7) T_7(Rb): the 30 K transition as clearly shown in χ measurements.

One problem, however, is that ρ at T_4(K) shows an inverse change compared with ρ at both T_4(Tl) and T_4(Rb). To reveal the nature of the transition T_4(K), we studied the solid solution system between $TlCu_7S_4$ and KCu_7S_4. X-ray diffraction measurements showed that these com-
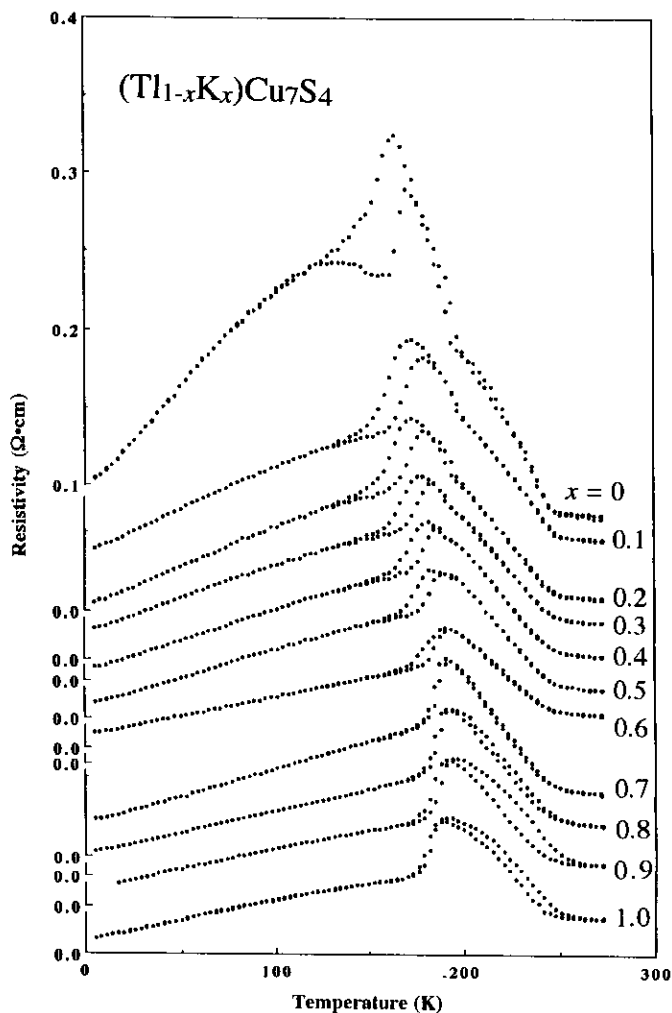

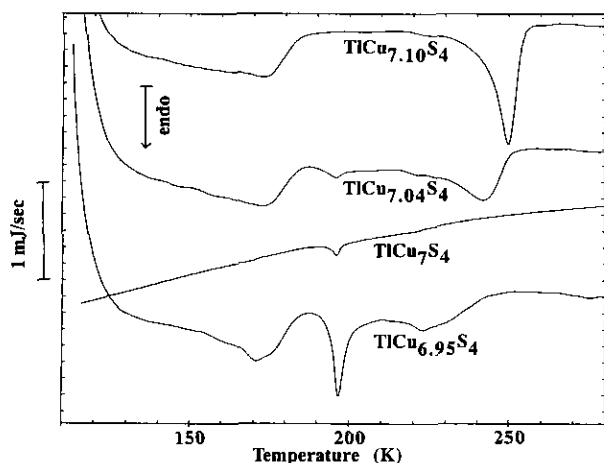FIG. 10. Temperature dependences of the resistivity ρ of $(Tl_{1-x}K_x)Cu_7S_4$ ($0 \leq x \leq 1.0$).

FIG. 11. DSC (differential scanning calorimetry) profiles on heating for the system $TlCu_{7+x}S_4$ $(-0.05 \leq x \leq 0.10)$. Measurements were carried out at the heating rate of 10 K/min.

pounds form a complete solid solution system. Figure 10 gives temperature dependences of ρ for the system $(Tl_{1-x}K_x)Cu_7S_4$ $(0 \leq x \leq 1.0)$. The temperature variations of ρ change continuously with the composition x; i.e., $T_4(Tl)$ appears to be continuously smeared with increasing K content, and T_5 (Tl) seems to come close to $T_4(K)$ with increasing K content. The latent heat observed in the DSC measurements also continuously increased with increased K content x. From the continuous changes of the transition temperature and ρ, it is assumed that the transitions $T_4(Tl)$ and $T_4(K)$ are substantially of the same type, and that $T_4(K)$ and T_5 (K) would occur almost simultaneously; thereby the inherent tendency to a jump of ρ on cooling at $T_4(K)$ would seemingly hide in a very narrow temperature range around 180 K. This speculation would be supported by the result that the latent heat of the transition $T_4(K)$ is quite large compared with that of T_4(Tl, Rb).

Figure 11 gives DSC data for the system $TlCu_{7\pm x}S_4$. The samples are the same ones used in the electrical measurements (see Figs. 8 and 9). Whangbo and Canadell claimed that the transitions in the present compounds are caused by an ordering of the Cu2 atoms in the tetrahedral chains (12). When the transitions are of the order–disorder type, the transition temperatures will show composition dependence (22). In the present results of the DSC, the transition temperature of $T_2(Tl)$ showed a slight increase with the increase of the Cu content, which is consistent with the results of ρ measurements as shown in Fig. 8. The latent heat of $T_2(Tl)$ also increases with increasing Cu content. These results suggest that $T_2(Tl)$, and possibly $T_2(K)$ and $T_2(Rb)$, are associated with a structural change such as the order–disorder transition. Thus, the transition $T_2(A)$ would be caused by a pairing distortion of the tetra-

hedral chains along the c axis, as suggested by Whangbo and Canadell (12), and as observed in the present ED pattern (see Figs. 6b and 7) exhibiting the doubled c axis. The transition temperature of $T_4(Tl)$ does not vary with the Cu content within experimental error, whereas the latent heat of $T_4(Tl)$ increases with decreasing Cu content, that is, with increasing conduction carriers. This shows that $T_4(Tl)$ would have an origin concerned with conduction carriers. The plausible candidate for $T_4(Tl)$, therefore, is the CDW transition which originates from the strong electron–phonon interaction. This speculation is consistent with the drop in χ on cooling across this transition, and with the additional satellite ED patterns, which resemble the patterns observed at the CDW transitions in Nb_3Te_4 (7, 23) and $In_xNb_3Te_4$ (8). But the semiconductivity above $T_4(Tl)$ may not be explained by this mechanism. In addition, the band calculation for the present compounds did not predict the CDW formation (12). Thus, one cannot rule out the possibility that another mechanism such as order–disorder transition is responsible for T_4. The transition $T_5(A)$ is accompanied by the change from semiconductive to metallic nature with decreasing temperature, which is typically shown by the drastic decrease of S values with decreasing temperature. Thus, this transition may be a metal–semiconductor transition (Mott transition) originating from strong electron correlation (24), as was observed in the pyrite system $Ni(S_{1-x}Se_x)_2$, which shows the semiconductor-to-metal transition with decreasing temperature (25, 26). The strong electron correlation effects were observed in many transition metal chalcogenides through various physical methods, e.g., photoelectron spectroscopy for NiS (27) and NMR measurements for V_3Se_4 and V_5Se_8 (28). These measurements may offer useful information on the electronic states in the present compounds.

Summarizing the above considerations, the origin of $T_2(A)$ is most likely the order–disorder transition, possibly concerned with Cu2 atoms in the tetrahedral chains. Although possible mechanisms were proposed for the origins of $T_4(A)$ and $T_5(A)$, there is no further corroborating evidence. Further, the origins for the other transitions are not clear. It is worth considering, thus, that atomic orderings or atomic displacements may play an important role in most of the transitions. More detailed analyses of structure as a function of temperature are needed.

CONCLUSIONS

Quasi-one-dimensional sulfides ACu_7S_4 $(A = Tl, K)$ with $(NH_4)Cu_7S_4$ type structure and a new isotypic sulfide $RbCu_7S_4$ were successfully prepared. The structure contains one-dimensional $[Cu_4S_4]$ columns. The columns are fused with double "CuS_3" tetrahedral chains, where the Cu sites are $\frac{1}{4}$ empty. It was found that the relatively high

conductivity is due to the presence of the vacancies of Cu or Tl atoms. Several phase transitions were observed in the temperature range from 3 to 450 K, which have characteristics common to all three compounds, and exhibit a distinct correlation between structure and physical properties. Such a large variety of successive phase transitions have not yet been found in other compounds. Two types of satellite patterns were successively observed on cooling in the electron diffraction measurements. The origin of $T_2(A)$ is most likely order–disordering of Cu2 atoms, but the origins of the other transitions are not definitely clarified. It is important to perform more detailed structural investigation, especially on the atomic displacements of Cu2 atoms, through low-temperature X-ray diffraction, Raman spectra, NMR studies, etc. Preparation of high quality single crystals is also important to solve these problems.

ACKNOWLEDGMENTS

REFERENCES

1. W. A. Little, *Phys. Rev. A* **134**, 1416 (1964).
2. J. Rouxel and C. Schlenker, in "Charge Density Waves in Solids" (L. P. Gor'kov and G. Grüner, Ed.), p. 15, North-Holland, Amsterdam, 1989.
3. A. Meerschaut and J. Rouxel, in "Crystal Chemistry and Properties of Materials with Quasi-One-Dimensional Structures" (J. Rouxel, Ed.), p. 205. Reidel, Dordrecht, 1986.
4. Z. Z. Wang, P. Monceau, M. Renard, P. Gressier, L. Guemas, and A. Meerschaut, *Solid State Commun.* **47**, 439 (1983).
5. C. Schlenker, J. Dumas, C. Escribe-Filippini, and H. Guyot, in "Low-Dimensional Electronic Properties of Molybdenum Bronzes and Oxides" (C. Schlenker, Ed.), p. 159. Kluwer Academic, Dordrecht, 1989.
6. Y. Ishihara and I. Nakada, *Solid State Commun.* **42**, 579 (1982); **44**, 1439 (1982).
7. T. Sekine, Y. Kiuchi, E. Matsuura, K. Uchinokura, and R. Yoshizaki, *Phys. Rev. B* **36**, 3153 (1987).
8. T. Ohtani, Y. Sano, and Y. Yokota, *J. Solid State Chem.* **103**, 504 (1993).
9. R. A. Berger and R. J. Sobott, *Monatsh. Chem.* **118**, 967 (1987).
10. Von G. Gattow, *Acta Crystallogr.* **10**, 549 (1957).
11. T. Ohtani, J. Ogura, M. Sakai, and Y. Sano, *Solid State Commun.* **78**, 913 (1991).
12. M.-H. Whangbo and E. Canadell, *Solid State Commun.* **81**, 895 (1992).
13. L. W. ter Haar, F. J. DiSalvo, H. E. Bair, R. M. Fleming, J. V. Waszczak, and W. E. Hatfield, *Phys. Rev. B* **35**, 1932 (1987).
14. R. M. Fleming, L. W. ter Haar, and F. J. DiSalvo, *Phys. Rev. B* **35**, 5388 (1987).
15. H. Sato, E. Igaki, T. Nakamura, T. Ban, and N. Kojima, *Solid State Commun.* **71**, 793 (1989).
16. H. Sato, N. Kojima, K. Suzuki, and T. Enoki, *J. Phys. Soc. Jpn.* **62**, 647 (1993).
17. H. Sato, Dissertation. Kyoto University, 1993.
18. F. Izumi, *Nippon Kessho Gakkaishi* **27**, 23 (1985) [in Japanese]; F. Izumi, in "The Rietveld Method" (R. A. Young Ed.), p. 236. Oxford Univ. Press, New York, 1993.
19. P. Mehrotra and R. Hoffman, *Inorg. Chem.* **17**, 2187 (1978).
20. L. Eriksson, P.-E. Werner, R. Berger, and A. Meerschaut, *J. Solid State Chem.* **90**, 61 (1991).
21. J. C. W. Folmer and F. Jellinek, *J. Less-Common Metals* **76**, 153 (1980).
22. For example, T. Ohtani, R. Fujimoto, H. Yoshinaga, M. Nakahira, and Y. Ueda, *J. Solid State Chem.* **48**, 161 (1983).
23. K. Suzuki, M. Ichihara, I. Nakada, and Y. Ishihara, *Solid State Commun.* **52**, 743 (1984); **59**, 291 (1986).
24. N. F. Mott, "Metal–Insulator Transitions." Taylor & Francis, London, 1990.
25. R. J. Bouchard, J. L. Gillson, and H. S. Jarrett, *Mater. Res. Bull.* **8**, 489 (1973).
26. P. Kwizera, M. S. Dresselhaus, and D. Adler, *Phys. Rev. B* **21**, 2328 (1980).
27. A. Fujimori, H. Namatame, M. Matoba, and S. Anzai, *Phys. Rev. B* **42**, 620 (1990).
28. Y. Kitaoka and H. Yasuoka, *J. Phys. Soc. Jpn.* **48**, 1460 (1980).